

# The intrinsically disordered C-RING biomineralization protein, AP7, creates protein phases that introduce nanopatterning and nanoporosities to mineral crystals. Supporting Information.

Eric P. Chang,<sup>†</sup> Jennie A. Russ,<sup>¶</sup> Andreas Verch,<sup>§</sup> Roland Kröger,<sup>§</sup> Lara A. Estroff,<sup>¶</sup> and John Spencer Evans<sup>†\*</sup>

<sup>†</sup>Laboratory for Chemical Physics, Department of Skeletal Biology, New York University New York, NY, USA.

<sup>¶</sup>Department of Materials Science and Engineering Cornell University, Ithaca, NY, USA.

<sup>§</sup>Department of Physics University of York, York, UK.

**KEYWORDS:** *Biomineralization / C-RING domain / protein phases / protein self-assembly / intrinsic disorder*

## Materials and Methods.

**Mineralization assays.** Chemically synthesized AP7 (MW = 7565 Da) was prepared and purified as described elsewhere.<sup>1</sup> Stock concentrations of AP7 were prepared using unbuffered deionized distilled water and lyophilized protein. Mineralization assays were adapted from published protocols<sup>2,3</sup> and were conducted by mixing equal volumes of 20 mM CaCl<sub>2</sub> \* 2H<sub>2</sub>O (pH 5.5) and 20 mM NaHCO<sub>3</sub> / Na<sub>2</sub>CO<sub>3</sub> buffer (pH 9.75) to a final volume of 500  $\mu$ L in sealed polypropylene tubes and incubating at room temperature for 1 min, 5 min, 15 min, and 1 hr.<sup>2</sup> An aliquot of AP7 stock solution was added to the calcium solution prior to the beginning of the assay, with final protein concentration = 100  $\mu$ M, identical to that utilized in previous aragonite nucleation studies.<sup>1</sup> The final pH of the reaction mixture was measured and found to be approximately 8.0 - 8.2.<sup>2</sup> Mineral and protein deposits formed during the assay were captured on 5 x 5 mm Si wafer chips (Ted Pella, Inc.) that were placed at the bottoms of the vials. Upon completion of a mineralization assay, the Si wafers were rinsed thoroughly 3x with calcium carbonate saturated methanol and dried overnight prior to analysis.

**Scanning Electron Microscopy.** Imaging of the Si wafers extracted from the mineralization assays was performed using a Merlin (Carl Zeiss) field emission SEM (FESEM) using either an Everhart-Thornley type secondary electron detector (SE2) or an annular secondary electron detector (in lens) at an accelerating voltage of 2.0 kV and a probe current of 600 pA. Prior to analysis, samples were coated with iridium using a Cressington 208HR sputter coater with thickness controller attachment. X-ray microanalysis of the iridium coated Si wafers was performed using an Oxford Instruments EDS with integrated INCA software attached to the Merlin FESEM. To perform the

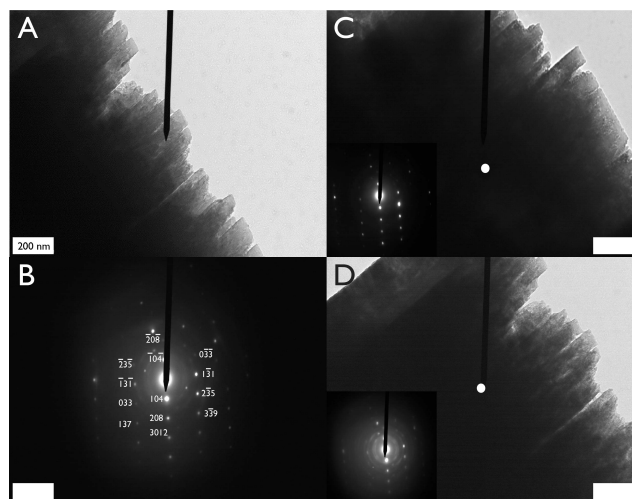


Figure S1: A) TEM image of crystal assembly. B) Corresponding single crystal electron diffraction pattern obtained from A), with hkl assignments corresponding to calcite. C), D) Representative TEM and electron diffraction data taken from other crystals assemblies showing calcite single crystal spot diffraction pattern (C) or overlapping single crystal and polycrystalline ring calcite diffraction patterns (D).

analysis, samples were lowered to a working distance of 8.0 mm and the acceleration voltage and probe current were increased to 10 k and 1.2 nA, respectively. Areas of interests were scanned for 100 seconds each.

**Transmission electron microscopy and selected area electron diffraction.** Crystals from the mineralization assays were extracted from the mineralization reaction vials using 0.2 micron filtered calcium carbonate saturated methanol and pipetted onto 200 square mesh gold grids coated with a formvar carbon film (Electron Microscopy Sciences, USA).<sup>2</sup> TEM and electron diffraction were performed using a Philips CM12

transmission electron microscope equipped with a tungsten filament electron beam source. All imaging and diffraction analyses were performed at 120 keV. A diffraction pattern of a polycrystalline gold standard was used as a calibration scale for all subsequently recorded diffraction patterns. The selected area diffraction patterns were analyzed and indexed using ImageJ and the JEMS software package.

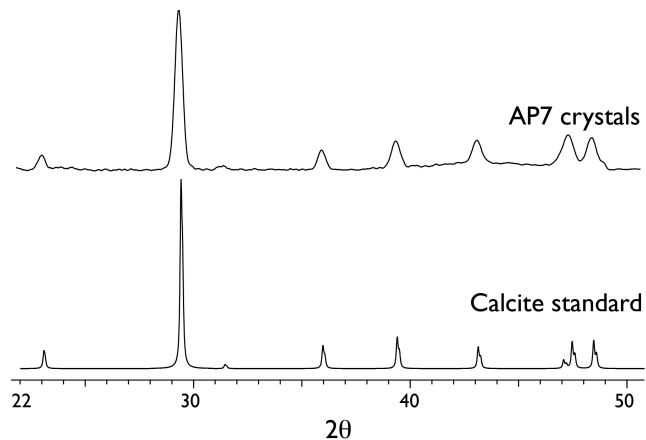


Figure S2: Micro x-ray diffraction powder pattern of bulk mineral deposits sampled from 1 hr AP7 mineralization assays. The standard x-ray diffraction spectra for calcite is presented for comparison.

**X-ray Diffraction (XRD).** Micro x-ray diffraction analysis was performed on the bulk mineral samples captured on Si wafers obtained from the mineralization reactions prior to being coated with iridium and analyzed with FESEM. XRD measurements were performed on a Bruker AXS D8 GADDS Powder X-ray Diffractometer equipped with a Vantec-2000 area detector. Samples were scanned over a broad range of  $2\theta$  values for 45 minutes each by oscillating and rotating the sample over a central area of approximately 1.8 x 1.8 mm on the Si wafer. The raw XRD data was processed, smoothed, and baseline subtracted using the Bruker AXS Eva DiffracPlus software program. These data were then compared to standard calcite, aragonite, and vaterite xrd powder pattern spectra for assignments.

**MicroRaman analysis of mineral deposits.** Si wafers containing washed and dried precipitated assay deposits were analyzed using a Renishaw InVia Raman microscope at Cornell University. Spectra were acquired under a 100X microscope objective with a laser excitation wavelength of 785 nm at 50% power (~4 mW), a 1200 line/mm grating, and a spot size of less than 1 micron.

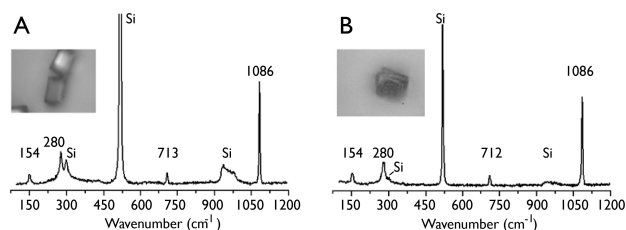


Figure S3: Representative Raman microscopy of mineralization assay crystals collected on Si wafers from (A) control and (B) AP7 mineralization assays, with corresponding light microscopic images of the deposits that were examined. Note that the Si wafer peaks do not overlap with any of the calcium carbonate – specific peaks. The Raman modes for synthetic aragonite, calcite and vaterite can be found in Table S1.<sup>4</sup>

Table S1: Raman band assignments for CaCO<sub>3</sub> polymorphs

Mode	Calcite (cm <sup>-1</sup> )	Vaterite (cm <sup>-1</sup> )	Aragonite (cm <sup>-1</sup> )
Lattice	156, 283	118, 268, 301	154, 208, 273
$\nu_1$	1086	1074, 1089	1086
$\nu_2$	---	874	854
$\nu_3$	1435	1445, 1485	1462, 1574
$\nu_4$	713	738, 750	704, 717
Overtone	1749	1749	---

Adapted from reference 4. Legend to table:  $\nu_1$  = symmetric stretch;  $\nu_2$  = out-of-plane bending;  $\nu_3$  = asymmetric stretch;  $\nu_4$  = in-plane bending

**Focused Ion Beam Milling (FIB).** The analysis of internal crystal morphology was performed using a Zeiss Auriga Small Dual-Beam FIB-SEM. Samples prepared for SEM imaging on the Zeiss Merlin were compatible with the Zeiss Auriga. All samples were coated with additional iridium prior to performing FIB. A 30 kV gallium ion beam was utilized to mill for depths of 10 – 15 mm below the beam focal point at 1 nA for coarse milling and 120 pA for fine milling. The gallium ion beam was oriented perpendicular to the sample by tilting the sample stage to 54°. SEM images of cross-sectioned surfaces were obtained using a 2.0 kV, 600 pA electron beam and a secondary electron detector at a working distance of 5.0 mm. Images were taken shortly after cross sectioning to limit the exposure of the uncoated surfaces to the electron beam. Images of surfaces containing electron beam damage were created for comparison to images of undamaged surfaces but were not used for the purposes of discussion in this publication.

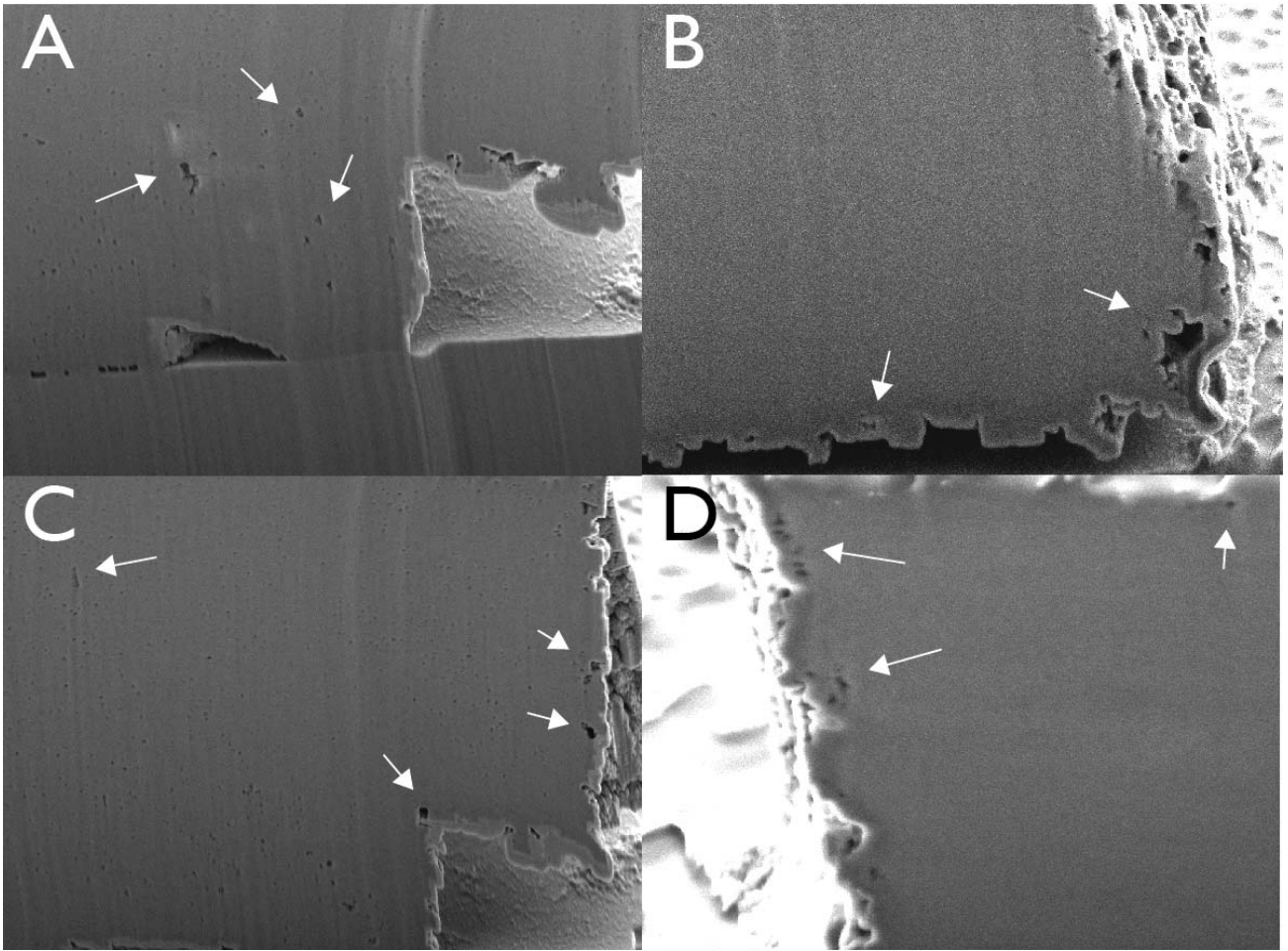


Figure S4. Series of higher magnification SEM images of FIB sectioned AP7 – modified calcite crystals, revealing nanometer-sized porosities or voids (arrows).

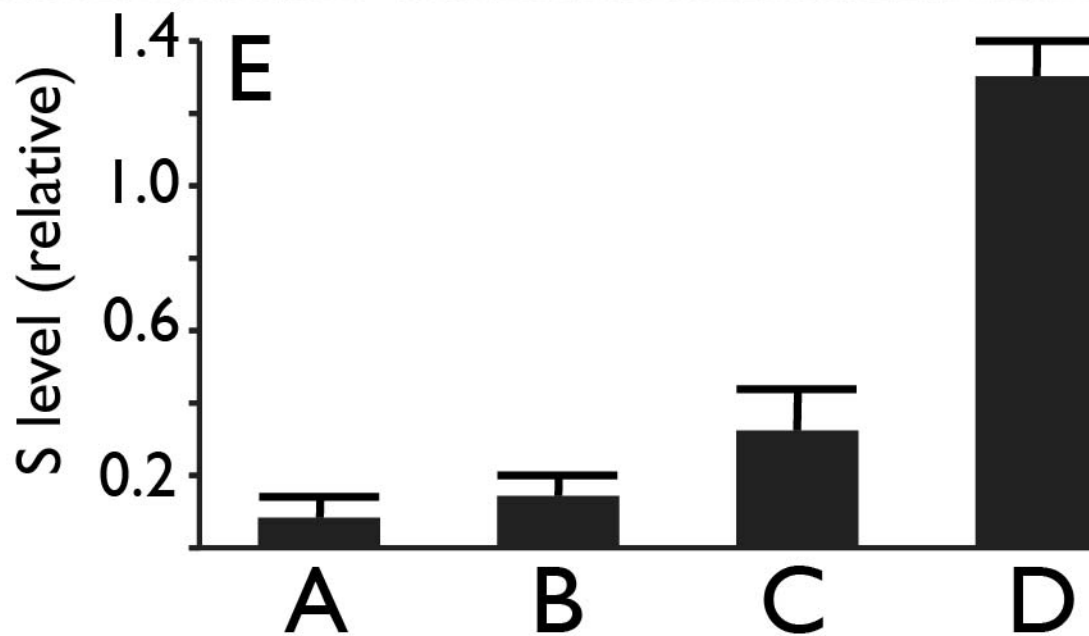
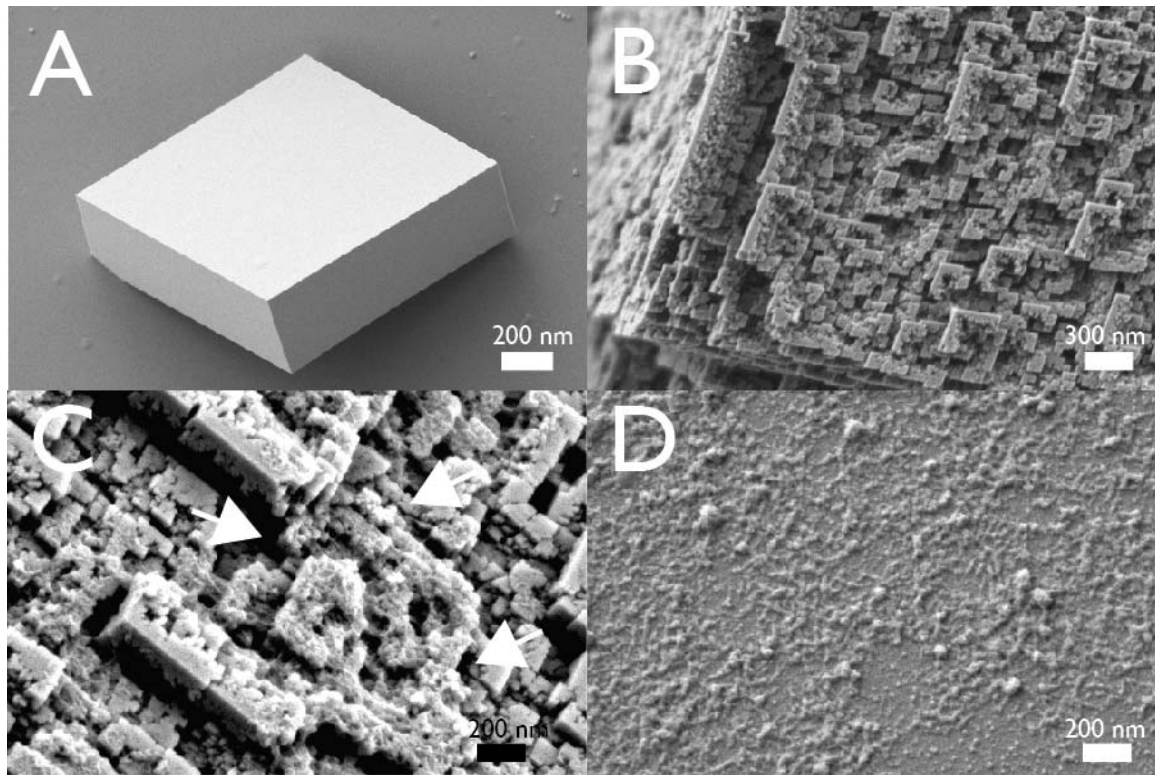


Figure S5. Representative SEM images of A) control crystals, B) AP7-modified crystals with no visual evidence of protein film at the surface; C) as per (B) but with evidence of protein phase deposits on exposed nanoparticle surfaces (arrows)(an enlarged image of this region is provided in Figure S6); D) AP7 protein deposits or phases captured on Si wafers during the mineralization assay. E) Corresponding EDX elemental S content of Ir-coated crystal surfaces and deposits shown in A-D.

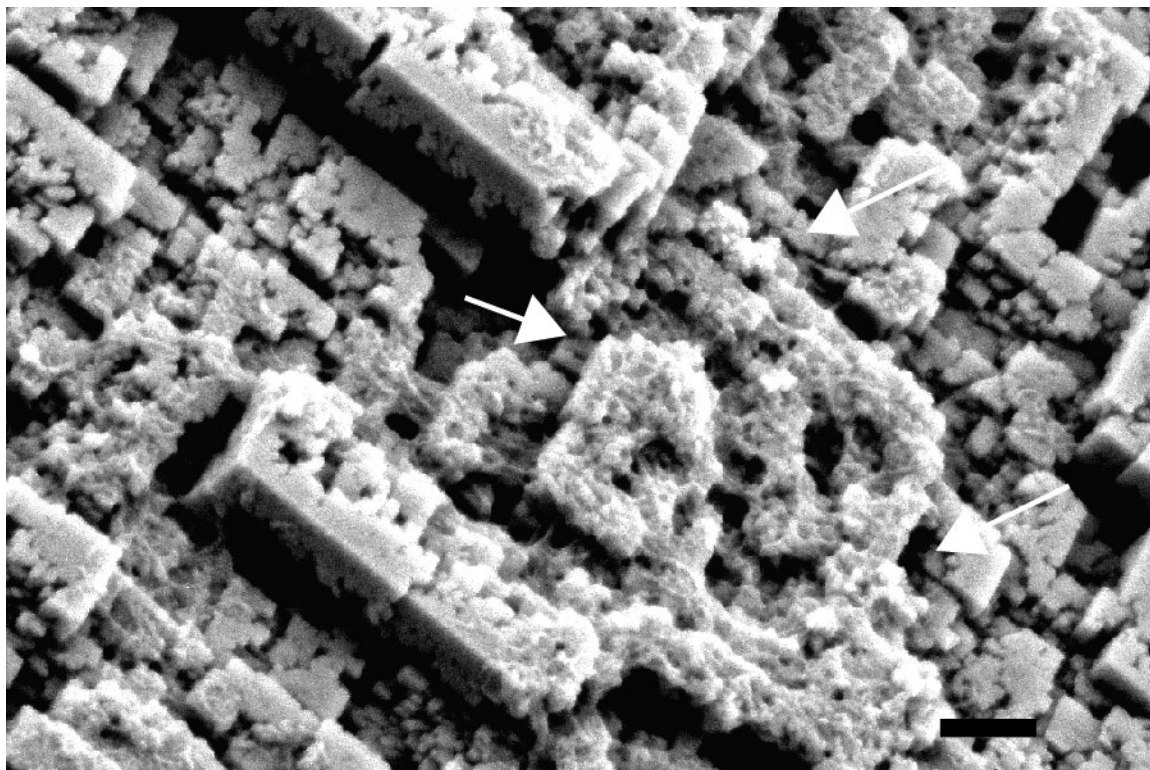


Figure S6. Enlargement of Figure S5C, which shows AP7 phases or coatings on the exposed horizontal surfaces of the nanoparticles (arrows). These phases present as “fuzzy” coatings on the crystals, with some evidence of bridging or connection with adjoining nanoparticle assemblies. Compare these “fuzzy” regions to the “clean” vertical sides of the nanoparticles which do not exhibit the AP7 phases. Scalebar = 200 nm.

## REFERENCES

- (1) Amos, F.F., Evans, J.S. (2009) *Biochemistry* 48, 1332-1339.
- (2) Perovic, I., Chang, E.P., Lui, M., Rao, A., Cölfen, H., Evans, J.S. (2014) *Biochemistry* 53, 2739-2748.
- (3) Stephens, C.J., Kim, Y.Y., Evans, S.D., Meldrum, F.C., Christenson, H.K. (2011) *J. Am. Chem. Soc.* 133, 5210-5215.
- (4) Ndao, M., Keene, E., Amos, F.A., Rewari, G., Ponce, C.B., L.A. Estroff, L.A., Evans, J.S. (2010) *Biomacromolecules* 11, 2539-2544.